



Thermally Induced Clamping Force Deviations in a Sensory Chuck for Thin-Walled Workpieces

Berend Denkena¹, Heinrich Klemme¹, Eike Wnendt¹ (✉), and Matthias Meier²

¹ Institute of Production Engineering and Machine Tools (IFW), Leibniz Universität Hannover, An der Universität 2, 30823 Garbsen, Germany
wnendt@ifw.uni-hannover.de

² HWR Spanntechnik GmbH, Luxemburg-Straße 5, 28876 Oyten, Germany

Abstract. Deviations between nominal and actual tolerances are a challenging problem during turning processes of thin-walled workpieces. One main cause of these deviations is the clamping force applied by the turning chuck to hold the workpiece. Due to the low stiffness of thin-walled workpieces, large workpiece deformations can occur even when clamping forces are low. For this reason, the clamping force needs to be precisely adjusted. A possible approach are chucks with integrated actuators. As a result of the more direct power transmission, these chucks have a potentially higher clamping force accuracy compared to conventional external actuation. However, integrated actuators are additional heat sources resulting in thermal loads and thermally induced deformations of the chuck components. Due to the resulting mechanical distortion of the chuck system, the precise adjustment of clamping forces is not possible. Thus, this paper evaluates the thermally induced clamping force deviations on a novel turning chuck with four integrated electric drives. A test bench is used to analyse both a single drive and the combination of all four drives regarding the temperature effect on the clamping force adjustability. A clamping force deviation of up to 26% is observed. Based on the measured chuck temperature, a compensation method is introduced leading to a clamping force accuracy of 96.9%.

Keywords: Power chucks · Sensory machine components · Clamping force

1 Introduction

Precision turning of thin-walled workpieces such as bearings, thin rings or turbines is of key importance in aerospace, automotive and medical applications [1]. One main cause of shape deviations is the clamping force applied by the turning chuck to hold the workpiece [2]. Due to the low stiffness of thin-walled workpieces, large workpiece deformations can occur even when clamping forces are low. For this reason, the appropriate clamping force has to be applied. To estimate the appropriate clamping force and thus to reduce shape deviations, FE-simulations or analytical calculations are used [3]. In this context, Sergeev et al. proposed an algorithm to adjust the appropriate clamping force by an external clamping cylinder leading to clamping force errors of 12–15% [4]. Since

clamping force error and shape deviation are related linear proportional, shape deviations can occur in the same amount. Therefore, an external actuated chuck is insufficient to ensure tight tolerances. To avoid shape deviations, chucks with integrated actuators were developed [5, 6]. However, these chucks are only suitable for certain workpiece diameters or manufacturing processes. In contrast, the most commonly used clamping device in turning are chucks with three or four jaws [7]. Jaw-chucks allow a flexible clamping of different workpiece diameters. As a result, jaw-chucks are universally used for turning. For these reasons, a novel jaw-chuck for universal workpiece clamping is presented in this paper. Due to its integrated electric drives, higher clamping force accuracy and sensitivity are expected compared to a conventional external actuation. The design of the sensory chuck is explained in Sect. 2. In addition, the actuating concept is proofed using a test bench. In Sect. 3, the compensation method of thermally induced clamping force deviations is presented and the achievable clamping force accuracy is analysed.

2 Sensory Chuck for Thin-Walled Workpieces

2.1 Sensory Chuck Design

The design of the sensory chuck is shown in Fig. 1. It is composed of two different modules: A standard four-jaw-chuck HWR VT-S031 and a module with four actuator units. Each of the four actuator units consists of a Harmonic Drive SE FHA-14C gear motor and a leadscrew. The leadscrew allows the transmission of rotational movement of the motor into a linear positioning movement required to actuate the 4-jaw-chuck. The leadscrews are mechanically connected in parallel via a coupling element to transmit the actuation force F_{act} . In addition, the leadscrew is designed for self-locking to maintain the clamping force F_{cl} even when power failures of the motor occur.

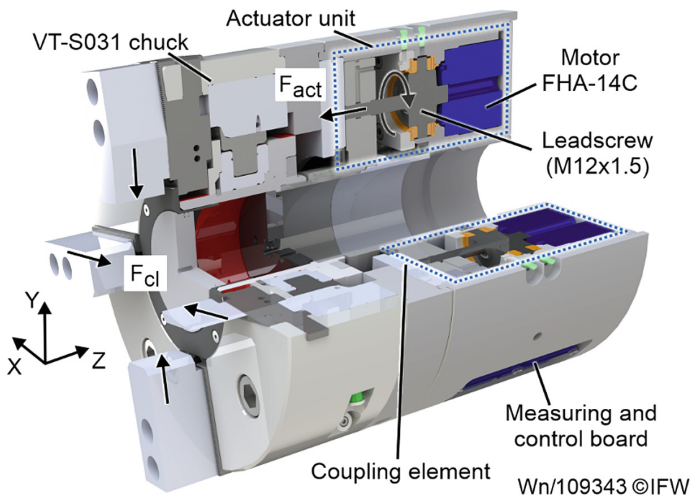


Fig. 1. Sensory chuck design

A total of four EJ7411 measuring and control boards from Beckhoff Automation GmbH & Co. KG are integrated into the chuck. Each EJ7411-module can measure and control the drive signals (motor torque M_m , angular position p) in a closed feedback loop. Based on the drive signals, the clamping force F_{cl} is calculated and adjusted considering a previously experimentally identified lookup table (see Sect. 3). Due to the self-locking leadscrew, clamping force adjustments are only possible by a feedforward control. For this reason, instationary variations of the clamping force (e.g. as a result of the cutting force) can not be considered.

The four-jaw-chuck HWR VT-S031 is designed to apply a maximum clamping force of $F_{cl,max} = 150$ kN. To achieve this force, each of the four actuator units has to provide an actuation force $F_{act} = 15$ kN. To proof the actuation concept, the test bench shown in Fig. 2a) is used. The test bench represents one of the four actuator units including one FHA-14C gear motor and the leadscrew. A force sensor based on strain gauges (Hottinger Brül & Kjaer U9C-50KN) measures the actuation force F_{act} . This sensor can measure forces in both +Z- and -Z- direction. During the experiments, different motor torques M_m are applied on the leadscrew and the resulting actuation force F_{act} is measured. As friction condition variations can lead to a significant deviation in axial forces for screws [8], two leadscrew lubricants (OKS265 and HLP32) are used to evaluate these correlations. The measurement is carried out at five different torques up to the limit for continuous loads of the motor ($M_m = 50\%$). The motor torque can be measured and adjusted by the EJ7411-module in percent of the peak motor torque.

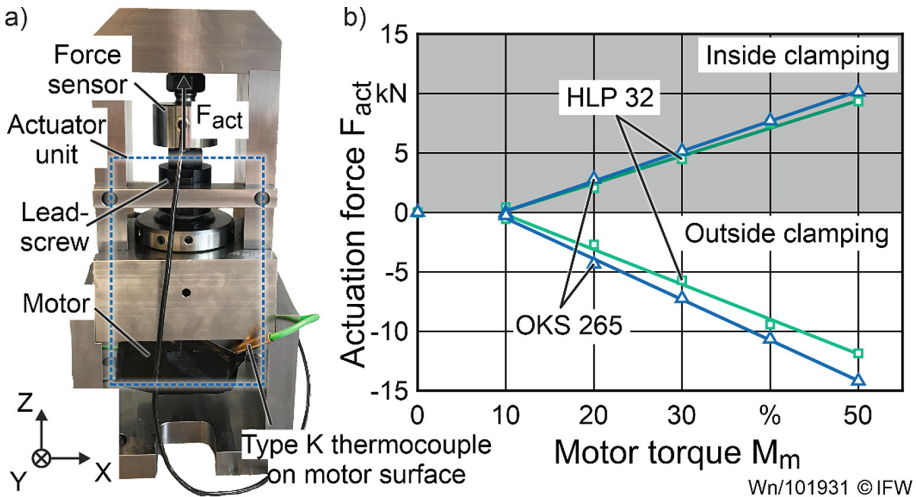


Fig. 2. Experimental setup to proof the actuation concept

The resulting correlations between the motor torque M_m and the actuation force F_{act} are presented in Fig. 2b). A linear proportional relationship between M_m and F_{act} can be observed. The highest force is $F_{act} = 14.5$ kN and occurs at the torque $M_m = 50\%$. For short-time ($t < 1$ s) peak torques, a maximal actuation force of $F_{act,max} = 18.3$ kN could be achieved (not shown in Fig. 2). Thus, the used actuation concept

provides sufficient high actuation forces to achieve a maximal clamping force of $F_{cl,max} = 150 \text{ kN}$. However, it can be seen that the actuation force also depends on the force direction due to the bearing friction moment between force sensor and leadscrew. Lower actuation forces can be achieved in + Z-direction which are used for inside clamping of workpieces. For inside clamping, the clamping force is increased by centrifugal forces during turning and thus lower actuation forces are sufficient for safe clamping. However, the results show higher actuation forces using OKS 265 lubricant. For outside clamping, the actuation force can be increased by up to 18.8% (8.5% for inside clamping) compared to HLP 30. Therefore, the OKS 265 lubricant is used for the prototype (see Sect. 3) to ensure high clamping forces.

2.2 Thermal Influences on the Actuation Force

For leadscrews, the actuation force highly depends on the friction coefficient μ in the thread [8]. In addition, high temperatures result in a generally high viscosity of the lubricant leading to a lower friction coefficient [9]. A lower friction coefficient increases the actuation force and thus the clamping force. Power losses of the motor are a heat source and could therefore affect the actuation force. To evaluate the influence of thermal losses on the actuation force, a reversing sequence of the motor was carried out with the test bench. A cycle of the sequence represents the clamping and machining of a typical ring-shaped workpiece. One cycle consists of a stepwise increase of the motor torque to $M_m = 50\%$ with subsequent constant torque for the time $t_{cl} = 10 \text{ s}$ (workpiece clamping and machining). For a complete cycle, the procedure is repeated in the opposite direction (workpiece removal and reloading). A total of $n = 1.000$ cycles are carried out while measuring the motor temperature with a type K thermocouple (Fig. 2a). In Fig. 3, the resulting correlation between the motor temperature ϑ and the actuation force

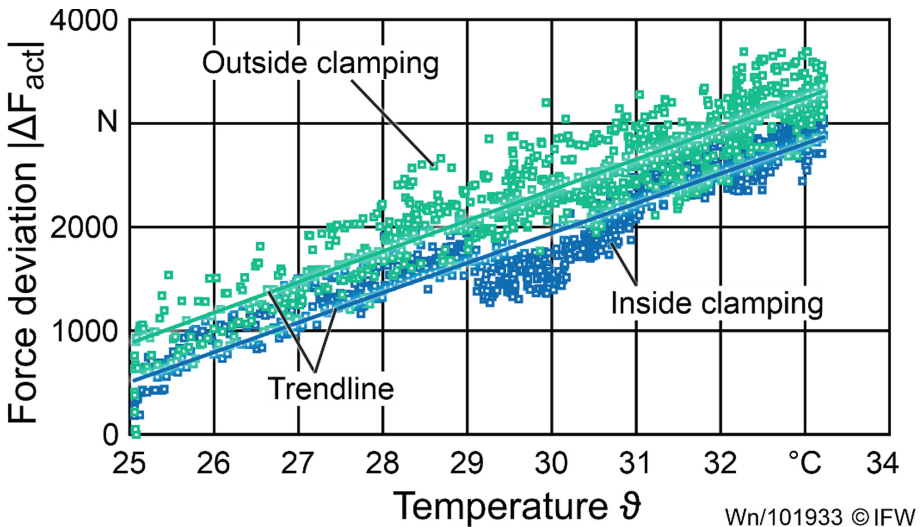


Fig. 3. Correlation between motor temperature and actuation force deviation

deviation $|\Delta F_{act}|$ is presented. This deviation is the difference between the measured force and the initial actuation force at a room temperature $\vartheta_0 = 25\text{ }^\circ\text{C}$. A linear proportional relationship between ϑ and $|\Delta F_{act}|$ can be observed. The highest actuation force deviation $|\Delta F_{act,max}| = 3.8\text{ kN}$ occurs for outside clamping at a temperature $\vartheta = 32.3\text{ }^\circ\text{C}$. This corresponds to a 26.2% increase in force compared to the initial actuation force $F_{act,0} = 14.5\text{ kN}$. Since the actuation force is proportional to the clamping force, thermally induced force deviations have a potentially significant influence on the clamping force. Therefore, this influence is evaluated in Sect. 3 using the assembled prototype.

3 Compensation of Thermally Induced Clamping Force Deviations

3.1 Clamping Force Adjustments with the Sensing Chuck Prototype

As shown in Sect. 2, thermal power losses of the actuation unit have a potentially significant influence on the clamping force. To evaluate this influence, the previously described experiments were repeated using the assembled prototype. First results showed, that the motor torque is not suitable to ensure a reliable clamping force adjustment. It is expected that highly non-linear friction between moving components of the chuck is the main cause of this issue. However, the measuring and control board of the chuck (see Fig. 1) provides an additional signal to adjust the clamping force: the angular position p . In order to verify whether the angular position allows a sufficiently high clamping force accuracy, the setup shown in Fig. 4a) was used. During the experiments, a reversing sequence of the motor was carried out. One cycle consists of a stepwise increase of the angular position up to the maximum achievable clamping force of the drives. A total of $n = 1.000$ cycles are carried out while measuring the motor temperature. During the experiments, the chuck temperature increased from $\vartheta_{chuck} = 23\text{ }^\circ\text{C}$ (room temperature) to a value of $\vartheta_{chuck} = 33\text{ }^\circ\text{C}$.

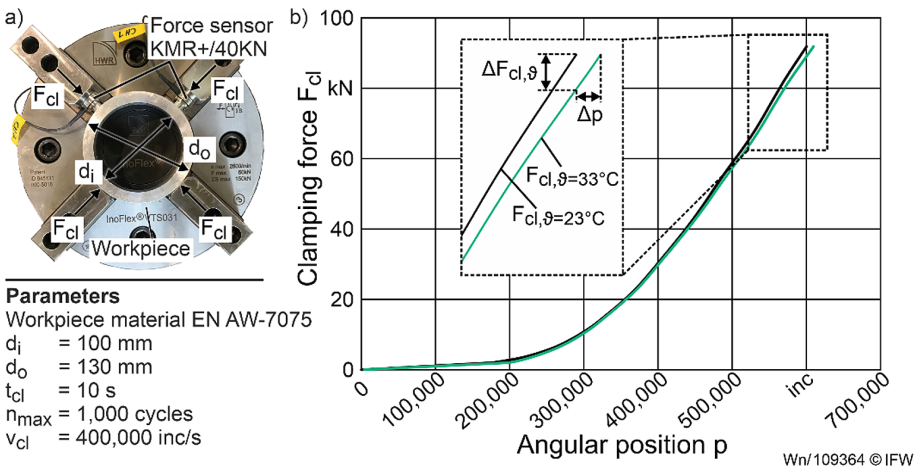


Fig. 4. Experimental setup and correlation between p and both F_{cl} and ϑ

In Fig. 4b), the resulting correlation between the angular position p and the clamping force F_{cl} is presented. In the diagram, the angular position is represented in increments. One increment (inc) represents the smallest detectable change in position. In addition, only the curve at the beginning ($\vartheta_{chuck} = 23\text{ }^{\circ}\text{C}$) and at the end ($\vartheta_{chuck} = 33\text{ }^{\circ}\text{C}$) of the measurements are shown. It can be seen that the clamping force also depends on the chuck temperature ϑ_{chuck} , resulting in small clamping force differences. The highest difference is $\Delta F_{cl,\vartheta} = 2.8\text{ kN}$ ($F_{cl,\vartheta=23\text{ }^{\circ}\text{C}} - F_{cl,\vartheta=33\text{ }^{\circ}\text{C}}$) and occurs at the position $p = 600,800\text{ inc}$. This corresponds to a relative clamping force error of $\Delta F_{rel} = 3.04\%$. In comparison, available clamping force measurement devices have a typical clamping force error of 3%. Therefore, the presented method of using the angular position for clamping force adjustments has a similar accuracy compared to specialized measuring devices on the market. To evaluate whether the error can be reduced further, a compensation method is proposed in Sect. 3.2.

3.2 Compensation of Clamping Force Errors

To evaluate whether the error can be reduced further, the identified correlation between angular position p , clamping force F_{cl} and chuck temperature ϑ are combined into a multidimensional lookup table. The lookup table was implemented into the EJ7411-modules and additional PT 100-sensors were integrated on the drives surface to monitor the chuck temperatures. Thereafter, the previous experiments were repeated. Based on five repetitions, the relative clamping force error ΔF_{rel} is calculated for each clamping force F_{cl} .

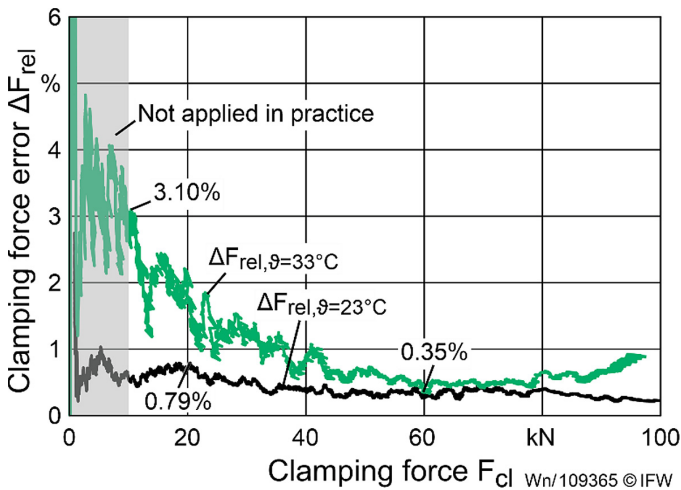


Fig. 5. Correlation between F_{cl} and both ΔF_{rel} and ϑ

In Fig. 5, the resulting correlation between the clamping force F_{cl} and the clamping force error ΔF_{rel} is shown. High errors ($\Delta F_{rel} > 3\%$) can be observed for clamping forces $F_{cl} \leq 10\text{ kN}$. According to [10], a minimum clamping force of $F_{cl,min} \approx 10\text{ kN}$

is required for safe clamping with the present chuck size. Below this clamping force, an uncontrollable workpiece release can occur. For this reason, clamping forces $F_{cl} \leq 10$ kN are not applied in practice. However, as the clamping force increases, smaller clamping force errors are achieved. The highest relative errors occur for $\vartheta_{chuck} = 33$ °C ranging from 0.35% to 3.10%. In addition, the highest absolute clamping force error is $\Delta F_{cl,max} = 862$ N at $F_{cl} = 97$ kN (not shown in Fig. 5). Compared to using only the angular position for clamping force adjustments (see Fig. 4, $\Delta F_{cl,\vartheta} = 2,800$ N), applying the lookup table reduces the clamping force errors by 69.3%. Especially for room temperature, the error is reduced to at least 0.79% respectively $\Delta F_{cl,max} = 325$ N ($F_{cl} = 80$ kN). Consequently, applying a lookup table allows a precise measurement and adjustment of the clamping force based on position and temperature signals of the drive.

4 Conclusion

This paper presents the design of a novel sensing chuck for clamping force measurement and adjustment. Thermal influences on the measurement accuracy are described and a compensation method is shown. With the compensation method, clamping force errors are reduced by 69.3%. Compared to common chucks ($\Delta F_{rel} \approx 10\%$), a lower clamping force error of 3.1% is achieved. Since the resulting shape deviation of thin-walled workpieces is proportional to clamping force [11], it is assumed that geometry deviations can be reduced to the same extent. Thus, future work aims to evaluate the machining tolerance achieved in cutting processes. In addition, further possible influences on the chuck accuracy (e.g. workpiece diameter, clamping position) will be investigated.

Acknowledgements. The results presented were obtained within research project “CyberChuck” (02P18K601). The authors thank the Federal Ministry of Education and Research for funding this project.

References

1. Brinksmeier, E., Sölter, J., Grote, C.: Distortion engineering – identification of causes for dimensional and form deviations of bearing rings. *CIRP Ann.* **56**(1), 109–112 (2007)
2. Heisel, U., Kang, C.: Model-based form error compensation in the turning of thin-walled cylindrical parts. *Prod. Eng.* **5**, 151–158 (2011)
3. Manikandan, H., Chandra Bera, T.: Modelling of dimensional and geometric error prediction in turning of thin-walled components. *Prec. Eng.* **72**, 382–396 (2021)
4. Sergeev, A.S., Tikhonova, Z.S., Krainev, D.V.: Automated thrust force calculation of machine tool actuators in fastening and turning steels. *Proc. Eng.* **206**, 1148–1154 (2017)
5. Denkena, B., Hülsemeyer, L.: Investigation of a Fine Positioning Method in Lathes Using an Active Clamping Chuck, pp. 245–246. *euspen* (2015)
6. Khaghani, A., Cheng, K.: Investigation on an innovative approach for clamping contact lens mould inserts in ultraprecision machining using an adaptive precision chuck and its application perspectives. *Int. J. Adv. Manuf. Tech.* **111**, 839–850 (2020)

7. Fleischer, J., Denkena, B., Winfough, B., Mori, M.: Workpiece and tool handling in metal cutting machines. *CIRP Ann.* **55**(2), 817–839 (2006)
8. Lambert, T.H.: Effects of variations in the screw thread coefficient of friction on the clamping force of bolted connections. *J. Mech. Eng. Science* **4**(4), 401–406 (1962)
9. Bair, S., Jarzynski, J., Winer, W.O.: The temperature, pressure and time dependence of lubricant viscosity. *Tribol. Int.* **37**(7), 461–468 (2001)
10. DIN German Institute for Standardization: Lathe Chucks, without Through-hole; Technical Conditions of Delivery for Power Operated Lathe Chucks (1983)
11. Estrems, M., Carrero-Blanco, J., Cumbicus, W.E., de Francisco, O., Sánchez, H.T.: Contact mechanics applied to the machining of thin rings. *Proc. Manuf.* **13**, 655–662 (2017)

Open Access This chapter is licensed under the terms of the Creative Commons Attribution 4.0 International License (<http://creativecommons.org/licenses/by/4.0/>), which permits use, sharing, adaptation, distribution and reproduction in any medium or format, as long as you give appropriate credit to the original author(s) and the source, provide a link to the Creative Commons license and indicate if changes were made.

The images or other third party material in this chapter are included in the chapter's Creative Commons license, unless indicated otherwise in a credit line to the material. If material is not included in the chapter's Creative Commons license and your intended use is not permitted by statutory regulation or exceeds the permitted use, you will need to obtain permission directly from the copyright holder.

